

Shortening synthesis process of zirconium hydroxide as a hydrolysis product of sodium zirconate

Muzakky ¹, Herry Poernomo ¹, Devi Swasti Prabasiwi ², Rahmatika Alfia Amiliana ²

¹ Research Center for Mining Technology, National Research and Innovation Agency, Jl. Babarsari Postal Code 6101 ykbb, Yogyakarta 55281, Indonesia

² Deputy for Research and Innovation Infrastructure, National Research and Innovation Agency, Jl. Babarsari Postal Code 6101 ykbb, Yogyakarta 55281, Indonesia

Corresponding author: devi013@brin.go.id (Devi Swasti Prabasiwi)

Abstract: This research was focusing on shortening the process of Zirconium hydroxide ($Zr(OH)_4$) synthesis to get a more efficient process. In the earlier method, $Zr(OH)_4$ was produced through ZOC, which was the product of Na_2ZrO_3 reacted with HCl. While this study offers a new method to synthesize $Zr(OH)_4$ through the hydrolysis process of sodium zirconate (Na_2ZrO_3), removing the leaching step of Na_2ZrO_3 with HCl. The hydrolysis process of Na_2ZrO_3 was carried out in a multistage stirred reactor at 70 °C. The multistage hydrolysis process occurred in 13 stages with 4000 grams of feed and 890 liters of water. This process produced 2500 grams of $Zr(OH)_4$. Then the impurities analysis was done using UV-Vis and atomic absorption spectroscopy (SAA). The UV-Vis analysis was done to analyze Si concentration, while the atomic absorption spectroscopy (SAA) was done to analyze Na concentration. Si and Na concentrations could decrease to 23.98 $\mu\text{g/ml}$ and 1.05 $\mu\text{g/ml}$, respectively. The $Zr(OH)_4$ contained in the residue was characterized using X-Ray Diffractometer (XRD) and Fourier Transform Infrared Spectroscopy (FTIR). Then, the calcination process of $Zr(OH)_4$ was done at 300 °C and 400 °C for 1 hour, and characterized using XRD. The XRD result shows crystals of zirconium titanium oxide or srilankite, and SiO_2 crystals that are separated from ZrO_2 or TiO_2 crystals. Surface analysis was done using Scanning Electron Microscope – Energy Dispersive X-Ray (SEM-EDX), the result shows that the hydrolysis process at the 3rd, 7th, and 13th stages have different amorphous crystals with bright colors. At the 13th hydrolysis stage, Zr concentration increased to 63.38%, and Si concentration decreased. Thus, the shorter process of $Zr(OH)_4$ synthesis has been done successfully.

Keywords: zirconium hydroxide, hydrolysis, sodium zirconate

1. Introduction

The hazardous materials in the environment urgently need to be removed because of their harmful effect both on the environment and humans. The construction sector plays a major role in environmental damage because of its massive use of materials (Hussain et al., 2022; Kien et al., 2022; Long, 2021). These materials may have been intentionally released into the ambient air, including toxic industrial compounds (TICs) or chemical warfare agents (CWAs). Activated carbon is used as standard material for retrieving these materials in ambient air through adsorption. Unfortunately, activated carbon has many shortcomings in its application (Oudejans, 2014). Due to the widespread use of activated carbon, the waste of activated carbon becomes a problem. Saturated activated carbon could release harmful substances because of high temperatures (Ma et al., 2021). Recently, amorphous zirconium hydroxide compounds ($Zr(OH)_4$) have been introduced to replace activated carbon for absorbing toxic agents (Glover et al., 2012; Peterson et al., 2010; Peterson & Rossin, 2012; Singh et al., 2012). Researchers in the waste industry found out that $Zr(OH)_4$ can be used to recover uranyl ions in solution (Liu et al., 2015) and excess fluoride in drinking water (Dou et al., 2012). As there are many advantages of $Zr(OH)_4$, there is a need to produce this material using the most effective method.

The hydrolysis process of zirconium oxychloride (ZOC or $ZrOCl_2$) using NH_4OH has been known as a common method to synthesize zirconium hydroxide ($Zr(OH)_4$), although the process has been varied in different ways. Synthesis of $Zr(OH)_4$ from ZOC is loaded with chemicals because to produce ZOC itself, a sufficient amount of chloride acid (HCl) is needed. HCl and sodium zirconate (Na_2ZrO_3) are reacted to produce ZOC. While the Na_2ZrO_3 is obtained from the roasting process of zircon minerals using NaOH. Then the NH_4OH is used for hydrolysis process of ZOC to produce $Zr(OH)_4$. (Aghazadeh et al., 2012; Biswas, Habib, & Islam, 2010; Mondal & Ram, 2004; Subuki et al., 2020; Zhang & He, 2012; Zhukov et al., 2019). As there are a lot of steps, thus this process takes a lot of processing time. Waste also becomes an important issue in this process because of the use of chemicals.

To overcome the issue, this study offers a new method to synthesize $Zr(OH)_4$. In this method, the process to produce ZOC from Na_2ZrO_3 is removed. After Na_2ZrO_3 was obtained from the fusion of zircon minerals and NaOH with a mole ratio of 1:4, then Na_2ZrO_3 enters the multistage hydrolysis process using water (H_2O). The synthesis of $Zr(OH)_4$ was carried out using stirred reactor equipped with temperature control. The reaction of zircon minerals roasting is as follows (Beyer et al., 1954; Biswas, Habib, Karmakar, et al., 2010):



Furthermore, Na_2ZrO_3 gradually undergoes hydrolysis with excess H_2O to form $ZrO(OH)_2$ at $pH > 9$, the reaction is as follows (Mondal & Ram, 2004):



If the hydrolysis process is continued until the pH is less than 7.5, then $Zr(OH)_4$ is formed with the reaction (Yamagata et al., 2008):



The comparison of the previous and new methods to produce $Zr(OH)_4$ can be seen in Fig. 1. By

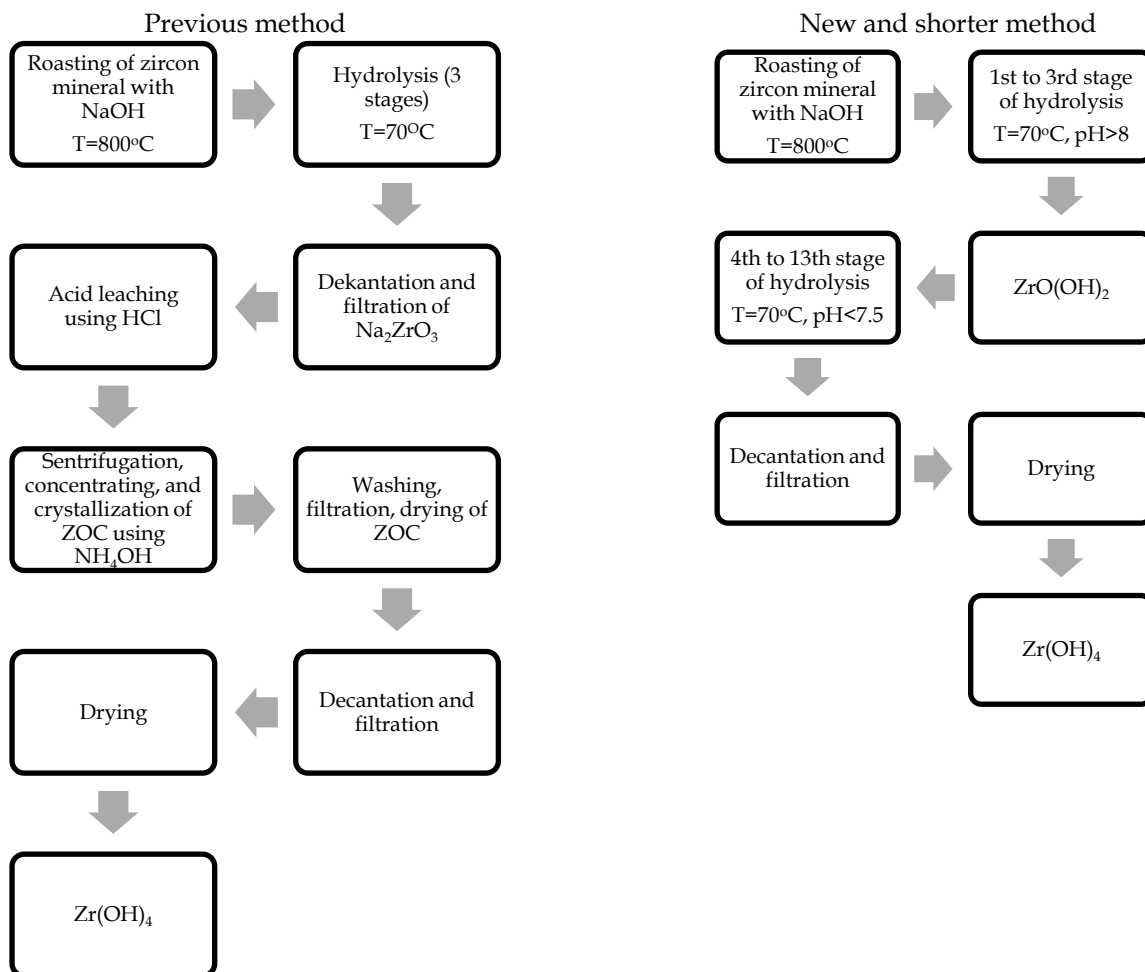


Fig. 1. The previous and new methods of $Zr(OH)_4$ synthesis

using the new method, it is expected that high product efficiency will be obtained. Furthermore, fewer chemicals are used in the new method. So the study of finding new method to produce $Zr(OH)_4$ is needed. This study faced some challenges because the impurity of Si relatively high in the final product. To overcome this issue, some stages of hydrolysis process has been added to remove Si contain in the product.

2. Materials and methods

2.1. Materials

The roasting of zircon minerals with NaOH (mole ratio of 1:4) took place at a temperature of 700 °C, for 3 hours (Biswas, Habib, Karmakar, et al., 2010; Muzakky, 2019). The roasting product has been analyzed by XRF, the result is as follows:

Table 1. Element composition of zircon minerals roasting product

SiO ₂	CaO	TiO ₂	Fe ₂ O ₃	Y ₂ O ₃	SnO ₂	ZrO ₂	SnO ₂
17.44%	0.27%	0.44%	0.37%	0.27%	0.41%	75.42%	0.41%

2.2. Tools

A set of 90 L stirred reactor equipped with a temperature controller is the main tool for the reaction to take place. While, the pH meter, Fourier Transform Infrared spectroscopy (FTIR, ALPHA II MODULE ATR ZnSe), X-Ray Diffractometer (XRD, PANanalytical Aeris type DY844 equipped with 161039 databases), and X-Ray Fluorescence spectrometer (XRF, Malvern PANanalytical High-Performance ED-XRF Epsilon 4), Scanning Electron Microscope-Energy Dispersive X-Ray (SEM-EDX, Phenom Desktop ProXL), Atomic Absorption Spectroscopy (AAS, Agilent AA 50), and UV- Vis (APHA 2012 Section 4500 C) have been used as analysis instrument for identifying the product of this research.

2.3. Methods

The hydrolysis process involved 4000 grams of roasting product of zircon sand with NaOH and 90 L of water. This process took place in the stirred reactor for ± 7 hours at a constant temperature of 70°C. The result of the hydrolysis process was left overnight, then the pH was measured. The concentration of Na and Si in this solution was determined using AAS. The residue was taken as much as 50 grams for analysis, while the filtrate was taken as much as 40 L. Then, 50 L of water was added to the filtrate so that the volume was maintained at 90 L to continue the hydrolysis process for the second stage. The hydrolysis process for Na_2ZrO_3 continued until the (n) stage when the pH is less than 7.5.

3. Results and discussion

Hydrolysis is a chemical process where water molecules act to break chemical compounds. One of the many factors that affect hydrolysis is the volume of water and the pH of solution (Barnum, 1983; Yamagata et al., 2008). Therefore, the effect of pH and water volume on hydrolysis stage of Na_2ZrO_3 should be studied to optimize the hydrolysis process. Mole ratio of Zircon sand and NaOH used in the reaction (1) is 1:4, then the excess of NaOH was removed by water (Biswas, Habib, Karmakar, et al., 2010). The hydrolysis process was carried out in stirred reactor with 90 liters capacity at 70°C. This process occurred in 13 stages then pH was observed as a function of water volume. The results can be seen in Fig. 2, which shows that at the 7th hydrolysis stage, the pH was 9.5 and began to decrease steadily. Thus, the amount of Na_2SiO_3 and the remaining NaOH was estimated to decrease significantly. Based on reaction (3), $ZrO(OH)_2$ started to form when the $pH > 9$ (Mondal & Ram, 2004). Furthermore, after the pH dropped to 7.026 in the 13th stage, it was estimated that reaction (4) would take place and $Zr(OH)_4$ would be formed. This is in accordance with Dou who has synthesized $Zr(OH)_4$ which was carried out at $pH < 7.5$ (Dou et al., 2012).

To prove this assumption, the concentration of Na and Si as Na_2SiO_3 (soluble in water) was analyzed to represent the amount of Na_2ZrO_3 and NaOH. Thus, the hydrolysis stage can be observed as a function of Na and Si concentration. In Fig. 3, it can be shown that the concentration of Si (as

Na_2SiO_3) has increased in the 3rd to 5th hydrolysis stage. This is because Na_2SiO_3 has started to dissolve in the bulk feed (leaching of zircon with NaOH) into the water. However, Si concentration began to drop in the 6th hydrolysis stage. Therefore, based on reaction (2), Na_2ZrO_3 peaked on the 3rd to 5th hydrolysis (Biswas, Habib, Karmakar, et al., 2010). At the 6th hydrolysis stage, the formation of $\text{ZrO}(\text{OH})_2$ has occurred spontaneously as reaction (3) stated.

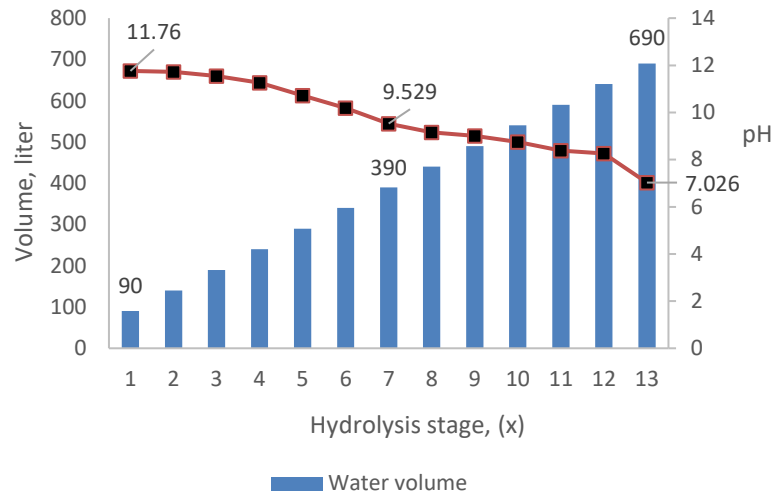


Fig. 2. The effect of pH and water volume on hydrolysis stage of Na_2ZrO_3

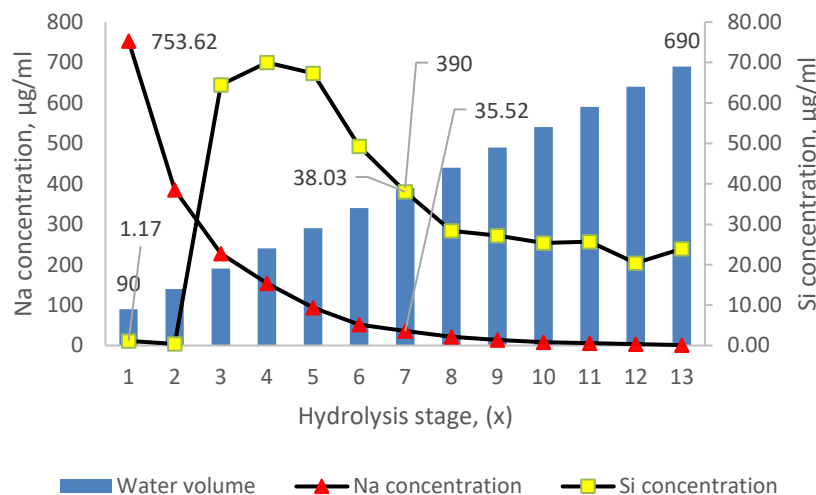


Fig. 3. Hydrolysis stage as function of Na and Si concentrations

When the hydrolysis process has reached the 7th stage (water volume = 390 L, Si concentration = 38.03 $\mu\text{g}/\text{ml}$), it is predicted that the formation of amorphous $\text{Zr}(\text{OH})_4$ has occurred although not entirely (based on reaction (4)) (Yamagata et al., 2008). Formation of $\text{Zr}(\text{OH})_4$ will continue to occur until the Si concentration reach 23.98 $\mu\text{g}/\text{ml}$ or the pH decrease to 7.026 (Fig. 2) (Dou et al., 2012).

In Fig. 3, it can be shown that the higher the hydrolysis stage, the Si concentration (as Na_2SiO_3) in the filtrate is decreasing. At the 13th stage of hydrolysis process (water volume = 690 L, pH = 7.026), Si is no longer detectable. Furthermore, the differences in the molecular structure of compounds between $\text{ZrO}(\text{OH})_2$ with $\text{pH} > 9$ and $\text{Zr}(\text{OH})_4$ with $\text{pH} < 7.5$ can be portrayed in the Fig. below (Huang et al., 2001).

Fig. 5 shows the XRD pattern of the Na_2ZrO_3 hydrolysis stage from 1st to 6th. XRD analysis was done using HighScore software and Inorganic Crystal Structure Database (ICSD). It can be seen in Fig. 5 that there are peaks at $2\theta = 17.9$, $2\theta = 35.7$, and $2\theta = 47.6$ which characterize as SiO_2 or Na_2SiO_3 with the symbol (∇). This compound is detected at the 1st to 5th hydrolysis stage. Furthermore, peaks at

$2\theta=26.8$, $2\theta=43.6$, $2\theta=55.4$, $2\theta=62.7$ and $2\theta=67.6$, which characterized as ZrO_2 or Na_2ZrO_3 with the symbol (\square), was found at all stages of hydrolysis. It indicates that the Na_2ZrO_3 compound is presented in the insoluble solid phase in the form of a paste. At the 7th hydrolysis stage, the $Zr(OH)_4$ crystals formed in amorphous phase. The $Zr(OH)_4$ crystal continued to form at the 8th to 13th hydrolysis stage. The results of the amorphous $Zr(OH)_4$ XRD pattern on the 12th and 13th hydrolysis stage can be seen in Fig. 6. It turns out that the phenomenon of the formation of $Zr(OH)_4$ in amorphous phase corresponds to the previous researchs (Aghazadeh et al., 2012; Meza Galvez et al., 2018; Peterson et al., 2010).

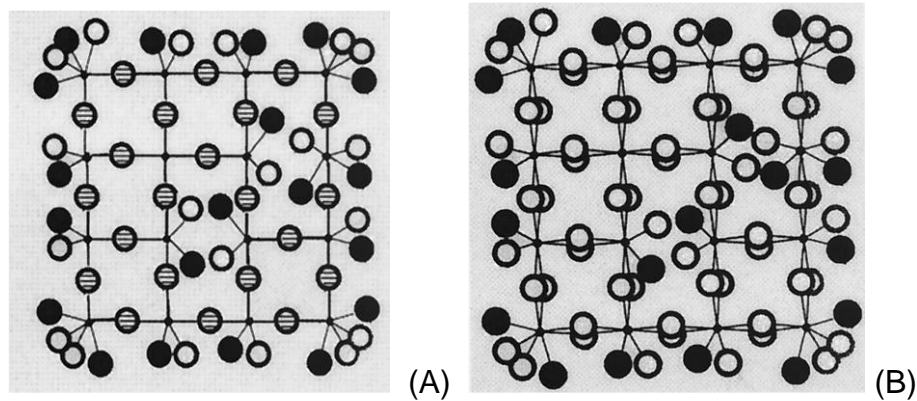


Fig. 4. (A) $ZrO(OH)_2$ as (*) Zr, (O) OH, (●) H_2O and (θ) Oxide bond (B) $Zr(OH)_4$ as (*) Zr, (O) OH, (●) H_2O

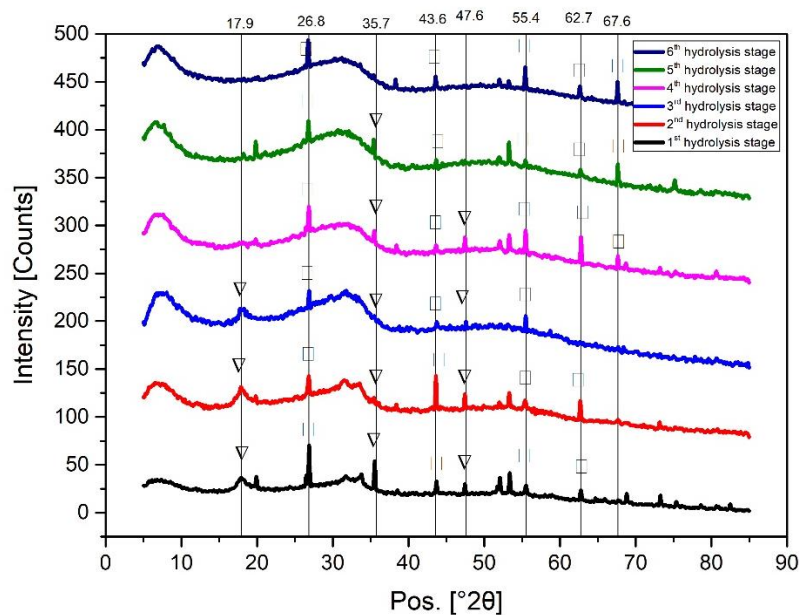


Fig. 5. XRD pattern of 1st to 6th hydrolysis stage shows Na_2SiO_3 (symbol ∇) and Na_2ZrO_3 (symbol \square)

In Fig. 7, the FTIR pattern of the Na_2ZrO_3 hydrolysis stage has been shown. At wavenumber of 3623.4 cm^{-1} , long horizontal peak was found and it belongs to the bond of the oxide-hydroxide group of zirconia ($Zr-O-OH$ in $ZrO(OH)_2$) (Wu et al., 2018). The oxide-hydroxide group bond is visible at the 1st to 5th hydrolysis stage, this indicates that the hydrolysis of Na_2ZrO_3 produces $ZrO(OH)_2$ as in equation (3).

At the 6th and 7th hydrolysis stage, the wavenumber of 3623.4 cm^{-1} was shifted toward 3445.6 cm^{-1} , which is the form of stretching vibrations of the O-H bonds (Aghazadeh et al., 2012; Peterson et al., 2010). The shift of those wavenumbers indicates the transformation of $ZrO(OH)_2$ to $Zr(OH)_4$. Furthermore, the wavenumber of 1644.1 cm^{-1} is a bond of water molecules vibration, which emphasizes the presence of Zr-OH group compounds (Aghazadeh et al., 2012; Dou et al., 2012;

Peterson et al., 2010). The reaction for the formation of $Zr(OH)_4$ from $ZrO(OH)_2$ in the hydrolysis process due to the increase in ionic strength with an excess of H^+ and OH^- ions is $ZrO(OH)_2 + H^+ + OH^- \rightarrow Zr(OH)_4$ (Mondal & Ram, 2004). While the wavenumber of 731.4 cm^{-1} is vibration from Zr-O bonds (George & Seena, 2012) and the wavenumber of 1000.1 cm^{-1} is generally a characteristic of Si-O-Si group symmetric stretching. However in this study, $ZrO(OH)_2$ and $Zr(OH)_4$ compounds are dominant in 1st to 7th hydrolysis stage, so it can be predicted that wavenumber of 1000.1 cm^{-1} can be mixed bonds between SiO_2 and ZrO_2 (Catauro et al., 2019). The wavenumber of 1000.1 cm^{-1} is a mixed bond of SiO_2 - ZrO_2 - TiO_2 (Bautista-Ruiz et al., 2014).

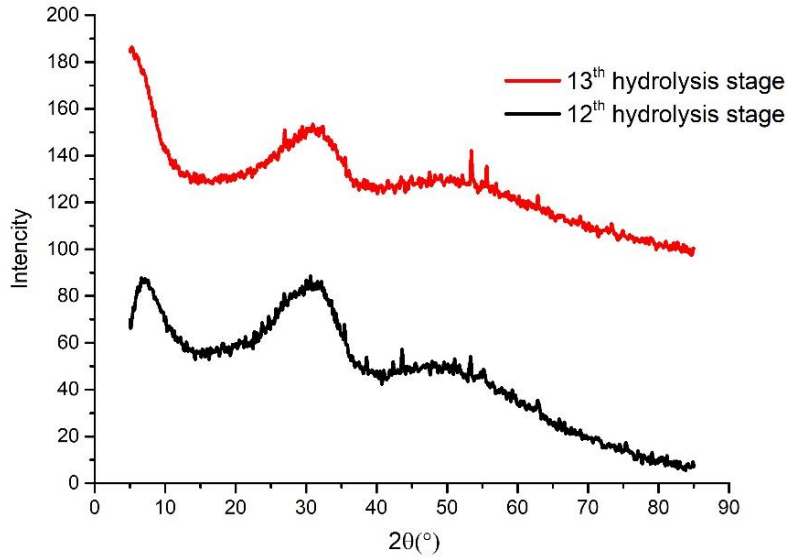


Fig. 6. XRD pattern of 12th and 13th hydrolysis stage shows amorphous $Zr(OH)_4$

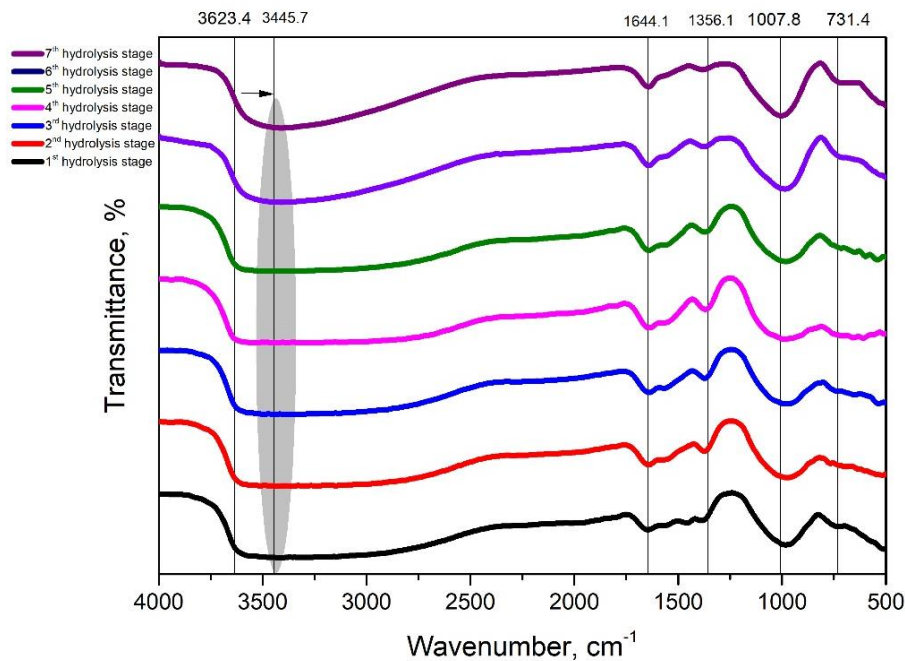


Fig. 7. $ZrO(OH)_2$ peak in FTIR pattern of 1st to 7th hydrolysis stage

Fig. 8 shows the conversion pattern of ZrO_2 , SiO_2 , and TiO_2 at each stage of the Na_2ZrO_3 hydrolysis process. Product conversion is calculated as solid conversion fraction (α) in each hydrolysis stage, the equation is as follows:

$$\alpha = \frac{\text{oxide in each stage of hydrolysis}}{\text{oxide in feed}} \quad (5)$$

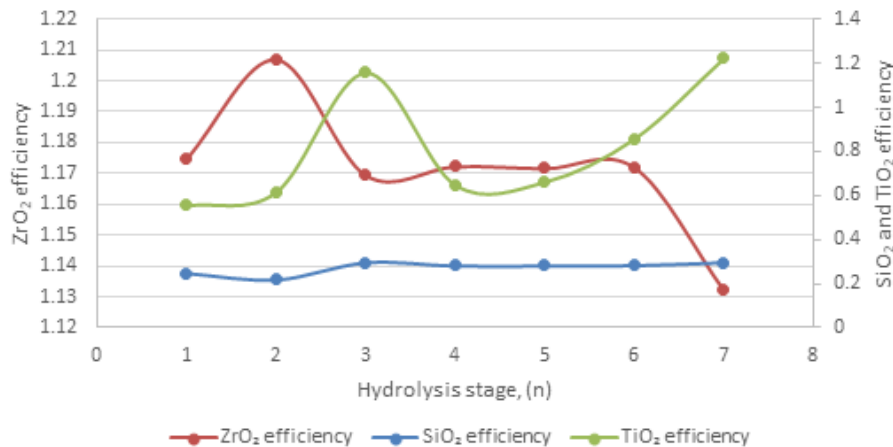


Fig. 8. Hydrolysis stage against ZrO₂, SiO₂ dan TiO₂ conversion

From Fig. 8, it can be seen that the conversion of ZrO₂ at the 2nd hydrolysis stage was increasing, then slightly stabilized but was decreasing at the 7th hydrolysis stage. This event shows that there has been a transformation from ZrO(OH)₂ to Zr(OH)₄ due to the hydrolysis process, resulting in some of the Zr(OH)₄ compound dissolves into the aqueous phase so that the efficiency of ZrO₂ decreases (Huang et al., 2001). The Zr(OH)₄ compound measured at 278 – 333 K could form amorphous crystals, and the solubility of log[Zr] tends to decrease at pH 7 (see Fig. 2) (Kobayashi et al., 2016). Meanwhile, based on the constant of the hydroxide complex formation, ZrO(OH)₂ has a log K of -1.5 which is much lower than log K of Zr(OH)₄ which is -9.6 (Barnum, 1983).

Fig. 8 also shows that the efficiency of SiO₂ at each stage of hydrolysis tends to be constant, but the efficiency of TiO₂ initially increases at the 2nd hydrolysis stage. Furthermore, the efficiency of TiO₂ was increasing significantly at the 7th hydrolysis stage, due to the possibility of ZrO₂-TiO₂ crystal bond in bulk Zr(OH)₄ compound starting to form. This prediction emphasizes the appearance of a wavenumber at 1000.1 cm⁻¹ in FTIR pattern (see Fig. 7) that represents ZrO₂-TiO₂ or ZrO₂-SiO₂ bond. This result is in accordance with previous research (Bautista-Ruiz et al., 2014). To justify this prediction, the amorphous Zr(OH)₄, which was the product from the 13th hydrolysis stage with a pH of 7.026 (see Fig. 6), was calcined for 1 hour at a temperature of 300 °C and 400 °C, respectively. Then the calcination products were characterized using XRD.

The red spectrum in Fig. 9 (1) shows the XRD pattern for Zr(OH)₄ calcination product from the 13th hydrolysis process or at pH 7.026 (see Fig. 6). The calcination occurred at a temperature of 300 °C for 1 hour. Fig. 9 (1) shows that there are 43.3% silicon oxide crystals, which form separate crystal groups. While the rest of the crystals is zirconium titanium oxide. But at a temperature of 300 °C between ZrO₂ and TiO₂ seemed to combine to form crystal groups called zirconium titanium oxide as much as 56.7%. Furthermore, Fig. 9 (2) is the result of the same product as number 1, but the calcination was carried out at a temperature of 400 °C and a fixed time of 1 hour. It turned out that in the calcination the silicon oxide crystals decreased to 42.9%, but the zirconium titanium oxide crystals increased to 57.1%. From the data in Figs. 9 (1) and 9 (2), although in the bulk Zr(OH)₄ there are several oxides such as ZrO₂, SiO₂, and TiO₂ (Fig. 8), there are still two dominant crystal groups. The first group is dominated by silicon oxide crystals, and the second is zirconium titanium oxide. Thus, in Fig. 7, especially at wave number 1000.1 cm⁻¹, it is predicted that the -O=Zr-Ti=O- group overlaps with the siloxane group -O-Si-O-.

Figs. 10, 11, and 12 are SEM images on the 3rd, 7th, and 13th hydrolysis product surfaces which were calcined at 300 °C. In Fig. 10, an amorphous crystal image is seen with the brightest color compared to the others. This is because the NaOH impurity which is described as the highest distribution of elements O, Si, Na, and Al (Bingzhuo et al., 2018). Zr(OH)₄ in the amorphous phase occurs at low temperatures and the crystal form will change along with the temperature increase (Ural et al., 2010). Furthermore, Fig. 11 indicates that the crystals are still in the amorphous phase and look darker than the 3rd hydrolysis stage. This is because each elemental impurity distribution of O, Si, Na, and Al has decreased. Then in Fig. 12, the crystals are still amorphous but have an elongated cylindrical shape,

with darker color than the others. However, in Fig. 12, it was possible to analyze the number of crystals formed by XRD compared to other hydrolysis methods (Fig. 9). In Fig. 12, the effect of the 13th hydrolysis increases the Zr element to 63.38%.

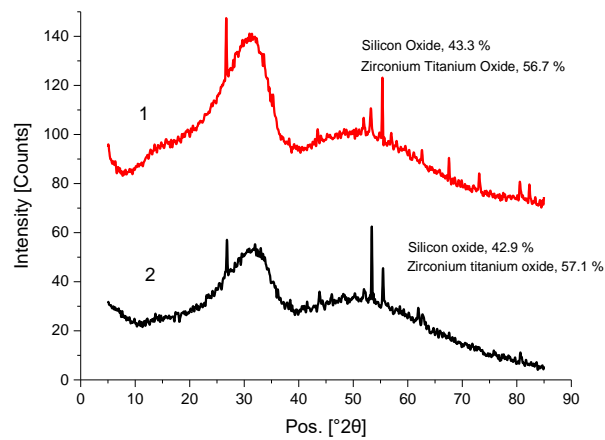


Fig. 9. XRD pattern of $Zr(OH)_4$ as product of hydrolysis at 13th stage

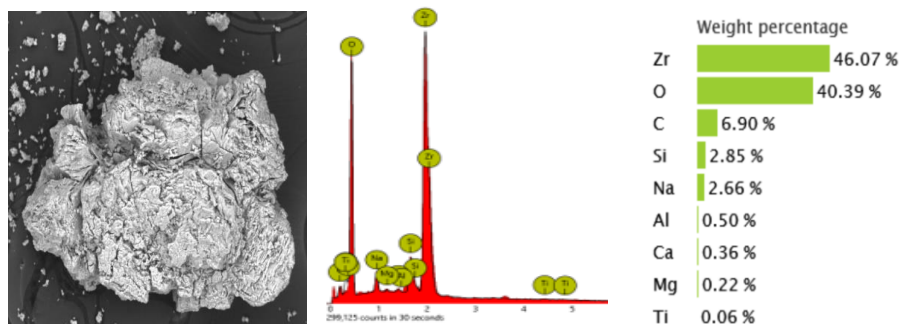


Fig. 10. SEM analysis of hydrolysis product at 3rd stage (300°C)

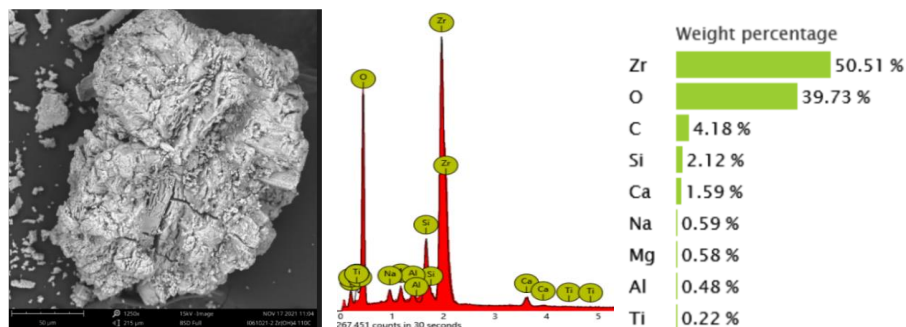


Fig. 11. SEM analysis of hydrolysis product at 7th stage (300°C)

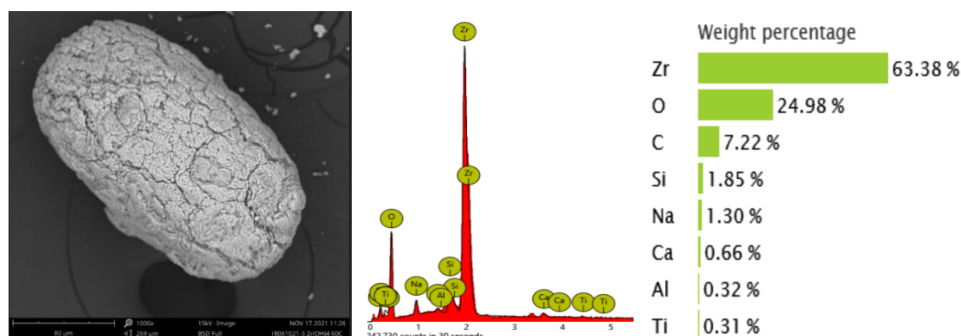


Fig. 12. SEM analysis of hydrolysis product of 13th stage (300°C)

4. Conclusions

The new and shorter process for zirconium hydroxide ($Zr(OH)_4$) synthesis has been studied and successfully done. The acid leaching process from previous method was removed so the $Zr(OH)_4$ was synthesized through hydrolysis process of Na_2ZrO_3 which is obtained from the alkaline roasting of zircon minerals. The hydrolysis process was carried out in a stirred reactor equipped with a temperature controller, in multistage mode. The hydrolysis process occurred in 13 stages which took up 4000 grams of feed and 890 liters of water. The yield of $Zr(OH)_4$ obtained from this process is 2500 grams. The higher the hydrolysis stage or pH, the concentration of Si and Na will decrease. The concentrations of Si and Na decreased to 23.98 $\mu\text{g/ml}$ and 1.05 $\mu\text{g/ml}$ at a pH of 7.026. XRD analysis can only be carried out at hydrolysis stages 1 to 7, because $Zr(OH)_4$ forms amorphous crystals. The shift of $ZrO(OH)_2$ to $Zr(OH)_4$ can be observed at hydrolysis stage 6 to 7 using FTIR, where the wave number 3623.4 cm^{-1} shifted towards 3445.6 cm^{-1} . The 13th stage of hydrolysis process produced $Zr(OH)_4$ at pH 7.026 then the product was calcined at 300 °C - 400 °C for 1 hour. The calcination process produced mixed crystals of zirconium titanium oxide or Srilankite and SiO_2 crystals which are separated from ZrO_2 and TiO_2 crystals. The results of the 3rd, 7th, and 13th hydrolysis stages turned out to have amorphous crystals that differed in the brightness of their colors. At the 13th hydrolysis stage, Zr concentration was increased to 63.38%, but Si concentration was decreased.

Acknowledgments

The authors would like to thank Rispro LPDP National Research Priority (PRN) PLTN-2 in 2021 through Agreement number 1/E1/III/PRN/2021 and SP DIPA 080.01.1.017290/2021 which helped a lot in terms of research funding. The authors are also very grateful to Janatul Firdausi, Seta Ayu Ningtyas, and Dewi Puspa Ariani who have helped a lot with laboratory work.

References

- AGHAZADEH, M., BARMİ, A. A. M., HOSSEINIFARD, M., 2012. *Nanoparticulates $Zr(OH)_4$ and ZrO_2 prepared by low-temperature cathodic electrodeposition*. Materials Letters. 73, 28–31.
- BARNUM, D. W., 1983. *Hydrolysis of Cations. Formation Constants and Standard Free Energies of Formation of Hydroxy Complexes*. Inorganic Chemistry. 22(16), 2297–2305.
- BAUTISTA-RUIZ, J., APERADOR, W., DELGADO, A., DÍAZ-LAGOS, M., 2014. *Synthesis and characterization of anticorrosive coatings of SiO_2 - TiO_2 - ZrO_2 obtained from sol-gel suspensions*. International Journal of Electrochemical Science. 9(8), 4144–4157.
- BEYER, G. H., SPINK, D. R., WEST, J. B., WILHELM, H. A., 1954. *Caustic Treatment of Zircon Sand*. Ames Laboratory ISC Technical Reports. 66.
- BINGZHUO, C., LU, Y., YING, C., HUAIQIN, Z., HAIFENG, X., FENG, H., 2018. *Effects of nano-zirconium hydroxide coating on resin bonding of 10-methacryloxy decyldihydrogen phosphate-conditioned*. West China Journal of Stomatology. 36(3), 252–256.
- BISWAS, R. K., HABIB, M. A., ISLAM, M. R., 2010. *A novel method for processing of Bangladeshi zircon: Part II: Leaching of zircon-caustic fused mass by hydrochloric acid*. Hydrometallurgy. 103(1–4), 130–135.
- BISWAS, R. K., HABIB, M. A., KARMAKAR, A. K., ISLAM, M. R., 2010. *A novel method for processing of Bangladeshi zircon: Part I: Baking, and fusion with NaOH*. Hydrometallurgy. 103(1–4), 124–129.
- CATAURO, M., BARRINO, F., BONONI, M., COLOMBINI, E., GIOVANARDI, R., VERONESI, P., TRANQUILLO, E., 2019. *Coating of titanium substrates with ZrO_2 and ZrO_2 - SiO_2 composites by sol-gel synthesis for biomedical applications: Structural characterization, mechanical and corrosive behavior*. Coatings. 9(3).
- DOU, X., MOHAN, D., PITTMAN, C. U., YANG, S., 2012. *Remediating fluoride from water using hydrous zirconium oxide*. Chemical Engineering Journal. 198–199, 236–245.
- GEORGE, A., SEENA, P. T., 2012. *Thermal studies on zirconium hydroxide gel formed by aqueous gelation*. Journal of Thermal Analysis and Calorimetry. 110(3), 1037–1041.
- GLOVER, T. G., PETERSON, G. W., DECOSTE, J. B., BROWE, M. A., 2012. *Adsorption of ammonia by sulfuric acid treated zirconium hydroxide*. Langmuir. 28(28), 10478–10487.
- HUANG, C., TANG, Z., ZHANG, Z., 2001. *Differences between Zirconium Hydroxide ($Zr(OH)_4 \cdot nH_2O$) and Hydrous Zirconia ($ZrO_2 \cdot nH_2O$)*. Journal of the American Ceramic Society. 84(7), 1637–1638.
- HUSSAIN, J., ZHANG, J., LINA, X., HUSSAIN, K., SHAH, S. Y. A., ALI, S., HUSSAIN, A., 2022. *Resource Assessment of Limestone Based on Engineering and Petrographic Analysis*. Civil Engineering Journal (Iran). 8(3),

421–437.

- KIEN, P. H., MONESAYKHAM, T., TRANG, G. T. T., 2022. *Molecular Dynamics Simulation to Investigate the Effect of Al₂O₃ Doping and Compression on the Structural Properties of Aluminium Silicate Glass*. Journal of Human, Earth, and Future. 3(2), 168–181.
- KOBAYASHI, T., UEMURA, T., SASAKI, T., TAKAGI, I., MORIYAMA, H., 2016. *The solubilities and solubility products of zirconium hydroxide and oxide after aging at 278, 313, and 333 K*. Radiochimica Acta. 104(3), 183–193.
- LIU, H., WANG, R., JIANG, H., GONG, H., WU, X., 2015. *Study on adsorption characteristics of uranyl ions from aqueous solutions using zirconium hydroxide*. Journal of Radioanalytical and Nuclear Chemistry.
- LONG, H. V., 2021. *Optimizing mixtures of alkali aluminosilicate cement based on ternary by-products*. Civil Engineering Journal (Iran). 7(7), 1264–1274.
- MA, Y., ZHANG, X., WEN, J., 2021. *Study on the Harm of Waste Activated Carbon and Novel Regeneration Technology of it*. IOP Conference Series: Earth and Environmental Science. 769(2).
- MEZA GALVES, J., OLEA MEJÍA, O., HERNÁNDEZ LÓPEZ, S., VIGUERAS SANTIAGO, E., CAMACHO LÓPEZ, M. A., 2018. *Amorphous Zr(OH)₄ to t-ZrO₂ transformed isothermally*. Superficies y Vacío. 31(3), 44–47.
- MONDAL, A., RAM, S., 2004. *Reconstructive phase formation of ZrO₂ nanoparticles in a new orthorhombic crystal structure from an energized porous ZrO(OH)₂xH₂O precursor*. Ceramics International. 30(2), 239–249.
- MUZAKKY., SUDARYADI., 2019. FTIR for controls of stoichiometry reaction of alkali fusion zirkon with NaOH. Ganendra Journal of Nuclear Science and Technology. 23(1), 19–27.
- OUDEJANS, L., 2014. Adsorption and Desorption of Chemical Warfare Agents on Activated Carbon : Impact of Temperature and Relative Humidity Adsorption and Desorption of Chemical Warfare Agents on Activated Carbon : Impact of Temperature and Relative Humidity. 261, EPA 600/R-14.
- PETERSON, G. W., ROSSIN, J. A., 2012. *Removal of chlorine gases from streams of air using reactive zirconium hydroxide based filtration media*. Industrial and Engineering Chemistry Research. 51(6), 2675–2681.
- PETERSON, G. W., WAGNER, G. W., KELLER, J. H., ROSSIN, J. A., 2010. *Enhanced cyanogen chloride removal by the reactive zirconium hydroxide substrate*. Industrial and Engineering Chemistry Research. 49(22), 11182–11187.
- SINGH, J., MUKHERJEE, A., SENGUPTA, S. K., IM, J., PETERSON, G. W., WHITTEN, J. E., 2012. *Sulfur dioxide and nitrogen dioxide adsorption on zinc oxide and zirconium hydroxide nanoparticles and the effect on photoluminescence*. Applied Surface Science. 258(15), 5778–5785.
- SUBUKI, I., MOHSIN, M. F., ISMAIL, M. H., FADZIL, F. S. M., 2020. *Study of the synthesis of zirconia powder from zircon sand obtained from zircon minerals malaysia by caustic fusion method*. Indonesian Journal of Chemistry. 20(4), 782–790.
- URAL, Ç., KÜLÜNK, T., KÜLÜNK, Ş., KURT, M., 2010. *The effect of laser treatment on bonding between zirconia ceramic surface and resin cement*. Acta Odontologica Scandinavica. 68(6), 354–359.
- WU, Y., CAI, T., ZHAO, W., CHEN, X., LIU, H., WANG, Y., RUSSEL, A. G., FAN, M., LIU, D., 2018. *First-principles and experimental studies of [ZrO(OH)]⁺ or ZrO(OH)₂ for enhancing CO₂ desorption kinetics-imperative for significant reduction of CO₂ capture energy consumption*. Journal of Materials Chemistry A. 6(36), 17671–17681.
- YAMAGATA, C., ANDRADE, J. B., USSUI, V., LIMA, N. B., PASCHOAL, J. O. A., 2008. *High purity zirconia and silica powders via wet process: Alkali fusion of zircon sand*. Materials Science Forum. 591–593, 771–776.
- ZHANG, R., HE, D., 2012. *Effect of alcohol solvents treated ZrO(OH)₂ hydrogel on properties of ZrO₂ and its catalytic performance in isosynthesis*. Journal of Natural Gas Chemistry. 21(1), 1–6.
- ZHUKOV, A. V., CHIZHEVSKAYA, S. V., PHYO, P., PANOV, V. A., 2019. *Heterophase Synthesis of Zirconium Hydroxide from Zirconium Oxychloride*. Inorganic Materials. 55(10), 994–1000.